INVESTIGATION OF THE HIGH ENERGY EXTENSIVE AIR SHOWERS

1. **EAS CORRELATED IN TIME**
2. **THE PECULIARITIES OF EAS MUON AND HADRON COMPONENT SPECTRA**
3. **GAMMA SHOWERS**

T.T.Barnaveli, T.T.Barnaveli (jr), N.A.Eristavi, I.V.Khaldeeva

Andronikashvili Institute of physics.

Tamarashvili st., 6, Tbilisi, Georgia

THE EAS BURSTS - HIGH ENERGY EXTENSIVE AIR SHOWERS CORRELATED IN TIME

T.T.Barnaveli, T.T.Barnaveli (jr), N.A.Eristavi, I.V.Khaldeeva
Andronikashvili Institute of physics.
Tamarashvili st., 6, Tbilisi, Georgia

A.P.Chubenko, N.M.Nesterova
Lebedev Physical Institute,
Leninsky av., 53, Moscow, Russia

This is a completely new result, obtained in 2009. It was published in ArXiv:0409.1944(2009)

The physics of this phenomenon is not clear yet.

So we are continuing the intensive study of it.

Summary

Bursts of **high energy EAS** intensity ("***SERIES OF EAS***), following each other in short intervals of time (1 – 5 minutes) were observed by means of Tien-Shan high mountain installation. Each series lasts <~ 0.5 hr.

For the size Ne >= 10**6 (primary energies of the order of 4•10**15 eV) was taken.

The additional condition was the presence at least of two EAS of Ne >10**7. The number of EAS in a series is from 4 to 9 events.

Five such series were found in the material treated (~250 days of pure time of installation run, more than 350 000 events in total).

- **Why the series? - If the primary particles are not gamma quanta, one can not identify the source by means of the EAS axes orientation distribution (even of very high energies) - the scattering of the primary particles on their way from the source to the Earth is too high, mainly due to deviation in the galactic magnetic fields.**

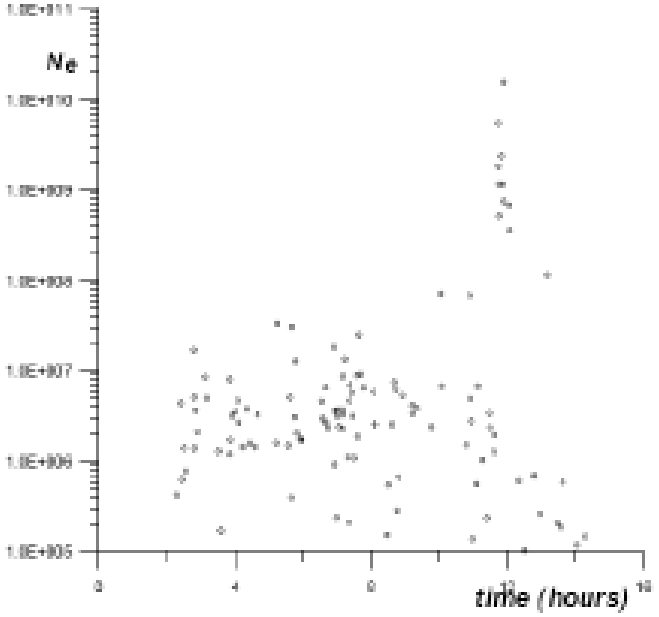

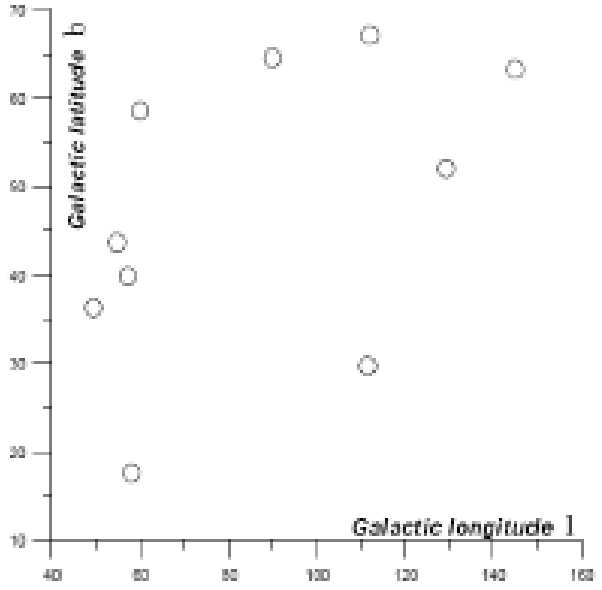

Fig. B. Series of 10 EAS, 13.11.1974, (run № 2333), <B> = 22.97°, <L> =65.88°, direction of maximal scattering 15.5° to the Galaxy equator plane

- **It is essential, that the frequency of the appearing of such series turned out to be much higher, than the probability of the occasional fluctuations in the succession of independent EAS. This probably is in favor of the commonality of their origin**.

- **For each EAS of each series, all the basic parameters are obtained:**

Observation date and time, age parameter S, galactic coordinates, coordinates of EAS axes relative to the installation center, energy release in the calorimeter and its distance from EAS axes, fitting the Nishimura-Kamata-Greisen (NKG) function.

- **EXPERIMENTAL RESULTS.**
- **ArXiv:0409.1944(2009)**
- For each of the series two graphs are given. On one of the graphs the position of the series on the dependence Ne(t) (built for the run under consideration) is represented. On the second graph is shown the distribution of the galactic coordinates of EAS axes directions for the EAS composing the given series. The graphs are followed by Tables, where the events included in the series are highlighted in bold.

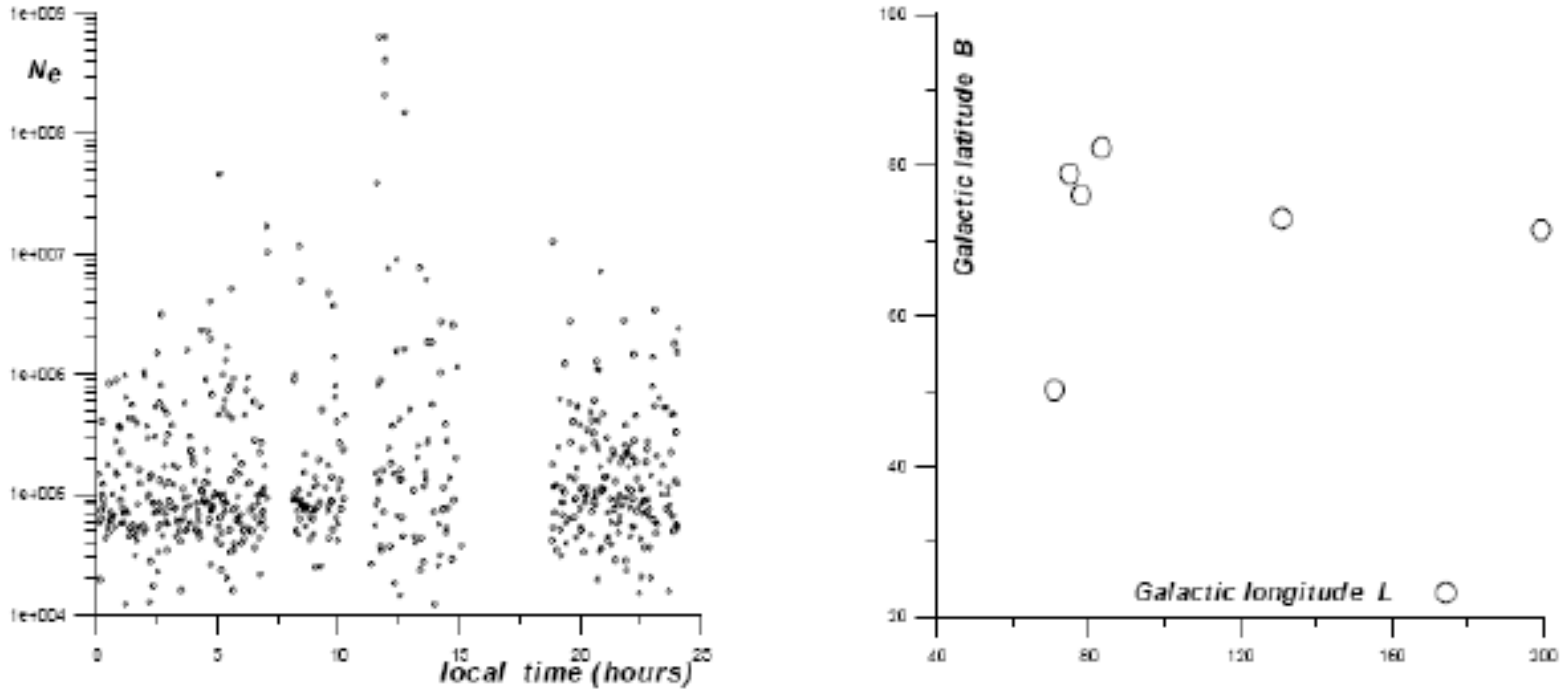

Fig. 3. Series № 3 (Run № 2751), 9 EAS, 15.10.1974, <B>=60.47°, <L>=132.45°, direction of maximal scattering 170.5° to the Galaxy equator plane. Probability of the occasional observation is $< 2 \cdot 10^{-17}$.

Table of data for series № 3 (Run № 2751)

LOC. TIME	N_E	E_0	B	L	S	EK	FF	X	Y	R
11.59	**$3.87 \cdot 10^{7}$**	**$4.4 \cdot 10^{16}$**	**58.25**	**87.07**	**0.113**	**0.386**	**$6.6 \cdot 10^{-2}$**	**12.5**	**1.1**	**13.4**
11.62	$8.94 \cdot 10^{4}$	$3.05 \cdot 10^{14}$	32.05	122.81	0.131	0.304	$8.2 \cdot 10^{-2}$	-3.8	6.8	4.0
11.63	$8.12 \cdot 10^{5}$	$2.08 \cdot 10^{15}$	76.92	135.54	1.882	$1.5 \cdot 10^{-5}$	$4.7 \cdot 10^{-2}$	-9.5	3.6	10.2
11.67	$2.88 \cdot 10^{4}$	$1.14 \cdot 10^{14}$	79.18	126.17	1.084	0.342	$5.3 \cdot 10^{-2}$	1.5	-2.2	3.7
11.67	$3.64 \cdot 10^{4}$	$1.39 \cdot 10^{14}$	53.22	40.72	0.997	1.071	$4.0 \cdot 10^{-2}$	2.6	1.4	1.8
11.67	$3.13 \cdot 10^{5}$	$9.07 \cdot 10^{14}$	56.72	141.1	0.873	0.295	$2.5 \cdot 10^{-2}$	-4.8	3.2	5.1
11.69	$1.29 \cdot 10^{5}$	$4.21 \cdot 10^{14}$	69.04	163.52	0.817	0.253	$2.6 \cdot 10^{-2}$	-3.2	-1.8	0.9
11.72	**$6{,}39 \cdot 10^{8}$**	**$6.86 \cdot 10^{17}$**	**23.07**	**174.15**	**0.176**	**0.587**	**$3.6 \cdot 10^{-2}$**	**8.3**	**-36.9**	**36.0**
11.75	**$2.58 \cdot 10^{6}$**	**$5.68 \cdot 10^{15}$**	**50.07**	**70.85**	**0.732**	**0.155**	**$1.6 \cdot 10^{-2}$**	**-5.9**	**22.6**	**15.1**
11.75	$3.32 \cdot 10^{4}$	$1.29 \cdot 10^{14}$	78.97	207.56	1.213	0.182	$6.2 \cdot 10^{-2}$	4.3	-2.0	4.5
11.75	$2.78 \cdot 10^{4}$	$1.10 \cdot 10^{14}$	76.22	103.14	0.869	0.445	$5.9 \cdot 10^{-2}$	-1.1	0.5	2.2
11.76	$3.69 \cdot 10^{4}$	$1.41 \cdot 10^{14}$	54.52	181.39	0.586	0.291	$6.0 \cdot 10^{-2}$	7.2	-6.4	7.6
11.78	$3.44 \cdot 10^{4}$	$1.33 \cdot 10^{14}$	55.58	134.05	0.808	0.283	$5.3 \cdot 10^{-2}$	3.9	-7.9	1.4
11.83	$1.58 \cdot 10^{5}$	$4.99 \cdot 10^{14}$	77.16	69.99	0.633	0.618	$2.0 \cdot 10^{-2}$	4.5	6.5	5.2
11.86	$7.12 \cdot 10^{4}$	$2.50 \cdot 10^{14}$	81.02	103.39	0.512	0.248	$3.4 \cdot 10^{-2}$	-6.4	1.6	6.0
11.92	**$1.68 \cdot 10^{8}$**	**$1.5 \cdot 10^{17}$**	**75.94**	**77.96**	**0.887**	**0.112**	**$7.49 \cdot 10^{-2}$**	**-1.3**	**0.9**	**1.5**
11.92	**$2.52 \cdot 10^{8}$**	**$2.15 \cdot 10^{17}$**	**78.81**	**74.93**	**0.420**	**0.214**	**$7.62 \cdot 10^{-2}$**	**1.0**	**3.7**	**3.2**
11.93	**$5.68 \cdot 10^{8}$**	**$4.25 \cdot 10^{17}$**	**82.22**	**83.33**	**0.087**	**$1.68 \cdot 10^{-5}$**	**$7.96 \cdot 10^{-2}$**	**1.1**	**-0.4**	**2.4**
11.93	**$2.52 \cdot 10^{8}$**	**$2.15 \cdot 10^{17}$**	**71.31**	**199.36**	**1.057**	**0.010**	**$7.44 \cdot 10^{-2}$**	**-0.2**	**1.5**	**4.6**
11.95	**$6.41 \cdot 10^{8}$**	**$4.7 \cdot 10^{17}$**	**72.83**	**130.91**	**1.159**	**$1.75 \cdot 10^{-5}$**	**$7.17 \cdot 10^{-2}$**	**-2.5**	**0.02**	**2.8**
12.04	**$7.56 \cdot 10^{6}$**	**$1.45 \cdot 10^{17}$**	**75.45**	**142.82**	**0.374**	**$1.76 \cdot 10^{-5}$**	**$3.45 \cdot 10^{-2}$**	**-66.6**	**36.6**	**75.4**

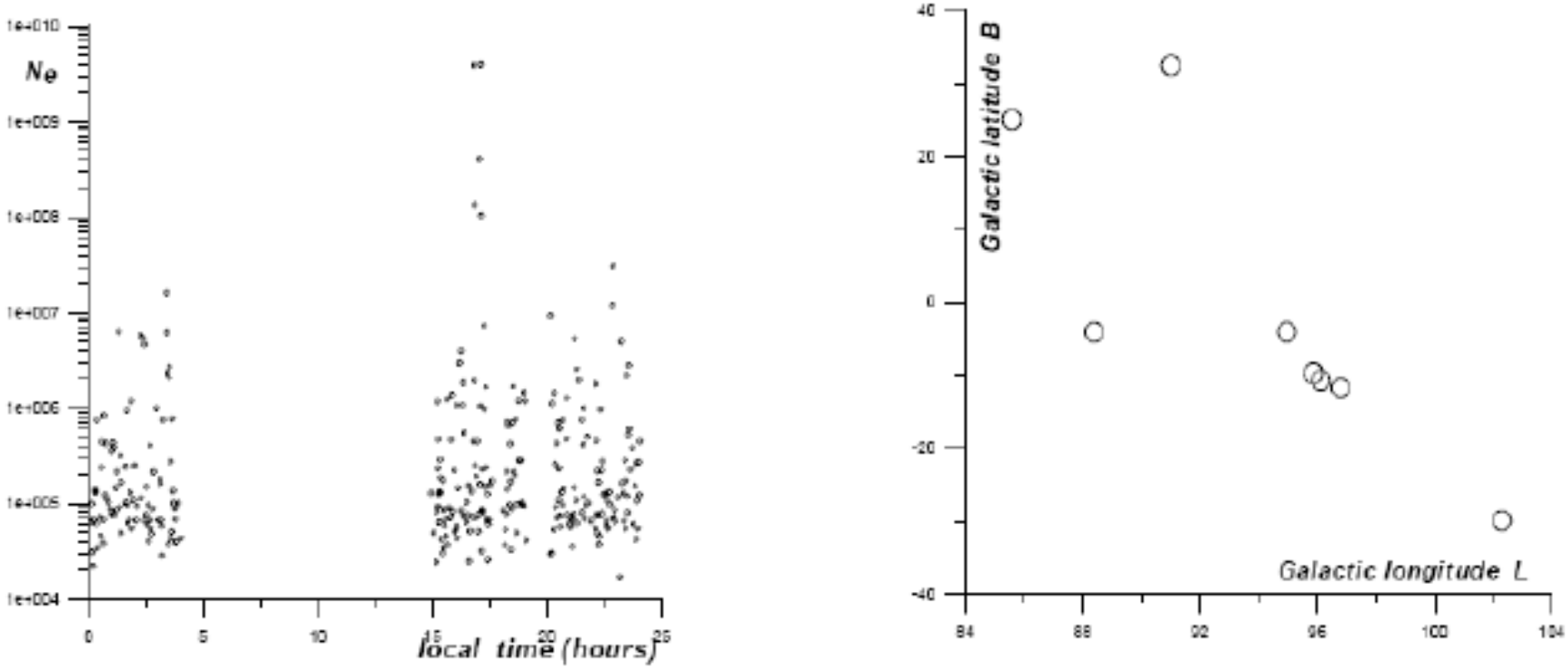

Fig.4. Series № 4 (Run № 2855), 8EAS, 25.12.1974, <B>=-6.05°, <L>=79.69°, direction of maximal scattering 94.5° to the Galaxy equator plane. Probability of the occasional observation is $< 10^{-19}$.

Table of data for series № 4 (Run № 2855)

LOC. TIME	N_E	E_0	B	L	S	EK	FF	X	Y	R
16.83	**$3.86 \cdot 10^{9}$**	**$3.28 \cdot 10^{18}$**	**-4.15**	**94.97**	**0.103**	**2.45**	**$7.8 \cdot 10^{-2}$**	**1.5**	**1.6**	**3.0**
16.85	**$3.49 \cdot 10^{6}$**	**$7.39 \cdot 10^{15}$**	**32.42**	**91.01**	**0.058**	**0.046**	**$5.9 \cdot 10^{-2}$**	**5.0**	**-5.7**	**7.4**
16.85	$3.67 \cdot 10^{5}$	$1.04 \cdot 10^{15}$	-28.36	133.02	0.154	0.005	$3.4 \cdot 10^{-2}$	11.7	8.4	9.8
16.87	**$2.66 \cdot 10^{8}$**	**$3.20 \cdot 10^{17}$**	**-4.17**	**88.39**	**0.816**	**3.10**	**$7.6 \cdot 10^{-2}$**	**-1.2**	**-1.7**	**2.9**
16.87	$1.42 \cdot 10^{5}$	$4.55 \cdot 10^{14}$	-12.02	91.47	0.798	0.653	$2.9 \cdot 10^{-2}$	5.6	-6.9	9.4
16.88	$2.47 \cdot 10^{5}$	$7.37 \cdot 10^{14}$	-24.07	89.23	0.650	0.210	$2.0 \cdot 10^{-2}$	2.8	-8.1	8.6
16.93	$2.51 \cdot 10^{5}$	$7.47 \cdot 10^{14}$	7.76	91.73	0.606	0.122	$3.6 \cdot 10^{-2}$	-13.3	-5.6	11.6
16.93	$1.29 \cdot 10^{5}$	$4.18 \cdot 10^{14}$	-25.01	52.59	0.320	$1.3 \cdot 10^{-5}$	$3.3 \cdot 10^{-2}$	-12.5	6.7	13.1
16.95	$6.18 \cdot 10^{5}$	$2.21 \cdot 10^{14}$	-8.92	136.11	0.889	0.074	$3.5 \cdot 10^{-2}$	-1.4	-5.2	7.7
16.95	$7.94 \cdot 10^{4}$	$2.75 \cdot 10^{14}$	2.66	86.66	0.881	0.001	$2.2 \cdot 10^{-2}$	-2.0	6.7	5.1
16.99	$2.14 \cdot 10^{4}$	$6.51 \cdot 10^{14}$	8.68	75.27	1.24	$1.6 \cdot 10^{-3}$	$2.6 \cdot 10^{-2}$	-10.3	0.01	6.1
16.99	$6.72 \cdot 10^{5}$	$1.76 \cdot 10^{15}$	-2.27	90.28	1.91	$9.5 \cdot 10^{-3}$	$6.0 \cdot 10^{-2}$	4.4	13.2	15.7
17.03	$5.04 \cdot 10^{5}$	$1.85 \cdot 10^{14}$	-13.97	101.84	0.571	0.232	$4.5 \cdot 10^{-2}$	-5.1	-0.9	4.0
17.05	$7.59 \cdot 10^{4}$	$2.64 \cdot 10^{14}$	-1.88	101.55	0.917	0.107	$2.5 \cdot 10^{-2}$	-2.7	-3.9	2.7
17.08	$7.11 \cdot 10^{4}$	$2.5 \cdot 10^{14}$	-4.79	88.65	1.064	0.156	$2.7 \cdot 10^{-2}$	-1.4	3.9	3.8
17.08	**$4.94 \cdot 10^{8}$**	**$5.49 \cdot 10^{17}$**	**25.01**	**85.60**	**0.175**	**0.88**	**$7.6 \cdot 10^{-2}$**	**3.5**	**0.5**	**5.9**
17.08	**$7.12 \cdot 10^{8}$**	**$7.54 \cdot 10^{17}$**	**-10.76**	**96.13**	**1.029**	**3.57**	**$7.2 \cdot 10^{-2}$**	**-2.7**	**1.5**	**2,8**
17.09	$1.57 \cdot 10^{5}$	$5.0 \cdot 10^{14}$	14.91	99.44	0.761	0.027	$2.4 \cdot 10^{-2}$	-2.8	7.3	7.8
17.12	**$1.03 \cdot 10^{6}$**	**$2.6 \cdot 10^{15}$**	**-29.98**	**102.31**	**1.23**	**0.065**	**$1.6 \cdot 10^{-2}$**	**-8.1**	**-1.1**	**6.3**
17.13	**$3.94 \cdot 10^{9}$**	**$3.4 \cdot 10^{18}$**	**-11.81**	**96.72**	**0.203**	**2.96**	**$7.7 \cdot 10^{-2}$**	**-8.1**	**8.7**	**11.0**
17.15	**$2.05 \cdot 10^{8}$**	**$2.6 \cdot 10^{17}$**	**-9.77**	**95.88**	**0.551**	**3.28**	**$7.4 \cdot 10^{-2}$**	**-0.7**	**-1.3**	**2.8**

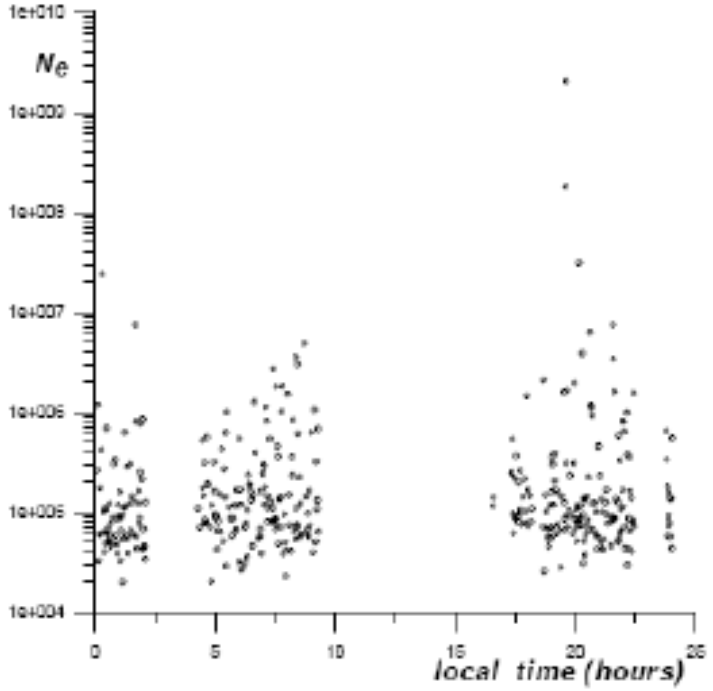

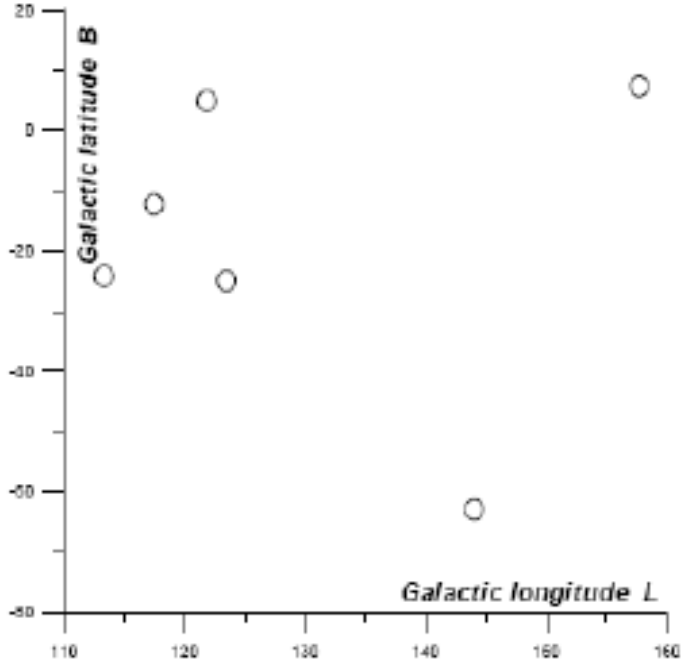

Fig. 5. Series № 5 (Run № 2856), 6 EAS, 26.12.1974, <B> = -13.42°, <L>=117.12°, direction of maximal scattering 110.5° to the Galaxy equator plane. Probability of the occasional observation is $< 6 \cdot 10^{-9}$.

Table of data for series № 5 (Run № 2856)

LOC. TIME	N_E	E_0	B	L	S	EK	FF	X	Y	R
19.53	**$1.57 \cdot 10^{6}$**	**$3.69 \cdot 10^{15}$**	**-24.95**	**123.46**	**0.795**	**0.547**	**$2.12 \cdot 10^{-2}$**	**-12.4**	**-5.4**	**11.9**
19.55	$1.23 \cdot 10^{5}$.	$4.04 \cdot 10^{14}$	-19.29	141.04	1.04	0.083	$3.85 \cdot 10^{-2}$	2.4	5.7	3.5
19.56	$8.5 \cdot 10^{5}$	$2.92 \cdot 10^{14}$	-19.21	76.29	0.91	1.12	$2.79 \cdot 10^{-2}$	-2.0	-2.5	1.8
19.58	$6.65 \cdot 10^{5}$	$1.35 \cdot 10^{14}$	-33.44	110.42	0.97	$1.67 \cdot 10^{-5}$	$5.06 \cdot 10^{-2}$	-13.2	6.2	14.5
19.59	4.11	$1.55 \cdot 10^{14}$	-3.18	122.15	0.74	0.35	$3.13 \cdot 10^{-2}$	3.7	2.8	3.8
19.60	**$5.39 \cdot 10^{8}$**	**$5.92 \cdot 10^{17}$**	**-24.22**	**113.33**	**0.217**	**0.524**	**$7.55 \cdot 10^{-2}$**	**-1.9**	**0.6**	**2.6**
19.60	$1.04 \cdot 10^{5}$	$3.47 \cdot 10^{14}$	-5.94	148.32	1.20	0.048	$3.76 \cdot 10^{-2}$	4.3	-3.4	6.3
19.62	**$6.04 \cdot 10^{9}$**	**$4.85 \cdot 10^{18}$**	**-12.26**	**117.47**	**0.213**	**3.55**	**$7.39 \cdot 10^{-2}$**	**-14.1**	**-10.3**	**16.5**
19.62	$6.55 \cdot 10^{4}$	$2.32 \cdot 10^{14}$	-9.74	143.02	0.769	$3.04 \cdot 10^{-3}$	$2.99 \cdot 10^{-2}$	-9.6	2.8	10.2
19.62	$5.05 \cdot 10^{4}$	$1.85 \cdot 10^{14}$	-46.24	66.81	0.914	$1.03 \cdot 10^{-5}$	$4.22 \cdot 10^{-2}$	-6.5	4.8	8.0
19.63	$5.38 \cdot 10^{5}$	$1.45 \cdot 10^{15}$	-23.42	116.70	0.688	0.044	$1.92 \cdot 10^{-2}$	-10.7	11.4	15.5
19.63	$7.43 \cdot 10^{4}$	$2.59 \cdot 10^{14}$	4.97	122.7	1.19	$2.94 \cdot 10^{-3}$	$4.44 \cdot 10^{-2}$	-9.3	1.4	8.0
19.65	$1.1 \cdot 10^{5}$	$3.65 \cdot 10^{14}$	-0.01	151.24	1.01	0.299	$2.84 \cdot 10^{-2}$	1.6	-3.3	4.5
19.65	$7.7 \cdot 10^{4}$	$2.68 \cdot 10^{14}$	4.39	107.99	0.658	$1.5 \cdot 10^{-5}$	$2.66 \cdot 10^{-2}$	6.6	5.6	9.9
19.66	**$1.63 \cdot 10^{6}$**	**$3.81 \cdot 10^{15}$**	**-62.96**	**144.02**	**0.202**	**$5.36 \cdot 10^{-3}$**	**$5.96 \cdot 10^{-2}$**	**-45.8**	**3.6**	**43.7**
19.68	$7.09 \cdot 10^{4}$	$2.49 \cdot 10^{14}$	-25.43	118.33	0.497	0.021	$3.64 \cdot 10^{-2}$	-5.5	-9.8	8.5
19.74	$1.02 \cdot 10^{5}$	$3.42 \cdot 10^{14}$	-20.96	127.44	0.843	$3.23 \cdot 10^{-3}$	$2.84 \cdot 10^{-2}$	9.19	-7.2	14.8
19.78	$2.31 \cdot 10^{5}$	$9.97 \cdot 10^{14}$	-58.39	117.39	0.761	0.025	$1.89 \cdot 10^{-2}$	-4.6	4.2	6.7
19.82	$9.13 \cdot 10^{4}$	$3.10 \cdot 10^{14}$	-9.77	108.68	0.99	1.93	$2.38 \cdot 10^{-2}$	-1.55	-3.2	2.0
19.91	$6.12 \cdot 10^{4}$	$2.19 \cdot 10^{14}$	-21.67	154.65	1.165	0.035	$3.80 \cdot 10^{-2}$	5.51	1.4	5.8
19.96	$3.04 \cdot 10^{5}$	$8.84 \cdot 10^{14}$	-24.72	146.23	0.813	4.81	$2.07 \cdot 10^{-2}$	-1.33	6.5	1.6
19.98	**$1.94 \cdot 10^{6}$**	**$4.43 \cdot 10^{15}$**	**7.37**	**157.69**	**0.662**	**0.185**	**$1.52 \cdot 10^{-2}$**	**3.8**	**22.2**	**14.6**
19.99	$8.42 \cdot 10^{4}$	$2.89 \cdot 10^{14}$	13.66	136.92	1.023	0.062	$3.01 \cdot 10^{-2}$	-7.8	1.6	4.7
20.01	$6.84 \cdot 10^{4}$	$2.41 \cdot 10^{14}$	-32.65	136.60	1.169	0.076	$3.39 \cdot 10^{-2}$	-1.6	1.1	1.6
20.05	$1.46 \cdot 10^{5}$	$4.66 \cdot 10^{14}$	-41.61	118.12	1.82	0.282	$2.99 \cdot 10^{-2}$	4.8	-6.7	7.5
20.05	$6.65 \cdot 10^{4}$	$2.35 \cdot 10^{14}$	0.77	134.65	0.955	0.156	$2.70 \cdot 10^{-2}$	2.7	4.4	3.9
20.06	$5.07 \cdot 10^{4}$	$1.86 \cdot 10^{14}$	-37.07	136.51	0.896	0.284	$3.21 \cdot 10^{-2}$	-2.0	1.5	1.8
20.08	$1.15 \cdot 10^{4}$	$3.81 \cdot 10^{14}$	-35.59	119.79	0.884	$8.31 \cdot 10^{-3}$	$2.18 \cdot 10^{-2}$	6.2	-7.7	8.6
20.09	$5.37 \cdot 10^{5}$	$1.95 \cdot 10^{14}$	-36.25	157.03	1.147	0.321	$5.07 \cdot 10^{-2}$	5.2	3.3	1.7
20.09	$9.44 \cdot 10^{4}$	$3.19 \cdot 10^{14}$	-14.61	118.45	0.674	0.029	$2.01 \cdot 10^{-2}$	-8.5	3.4	10.0
20.11	$8.12 \cdot 10^{4}$	$2.80 \cdot 10^{14}$	8.71	118.57	0.643	$4.82 \cdot 10^{-3}$	$2.61 \cdot 10^{-2}$	4.3	7.1	7.3
20.17	**$3.1 \cdot 10^{7}$**	**$4.94 \cdot 10^{16}$**	**4.91**	**121.84**	**0.207**	**0.256**	**$1.66 \cdot 10^{-2}$**	**29.9**	**-6.8**	**29.6**

- **Most urgent is to be aware that the registered phenomenon is not an imitation, namely that the EAS in series are true extensive air showers. One can bring three main arguments in favor of the registered EAS veritablity.**

- **1. There are in total 110 EAS in the time frames of all registered series (including the EAS of comparatively small energies). 100 of them are accompanied by the nonzero energy release in the ionization calorimeter.**
- **In addition, in 77 events there are distinct penetrating tracks in the calorimeter, in many cases multiple ones (pairs, threes) are registered, with the accompanying cascades.**
- **As an example, *the events in the calorimeter* for one of the series are shown on the next slide. There are several large nuclear cascades as well, two of them are shown further.**

19.42-A

19.70

19.72

19.73

19.77

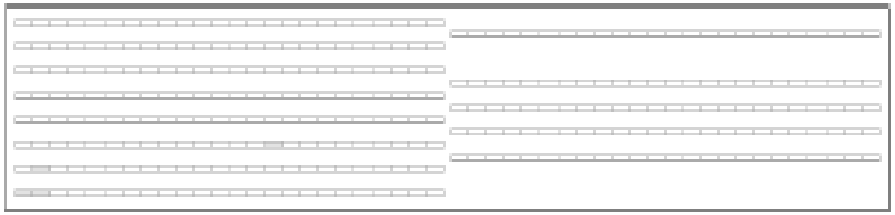

19.78

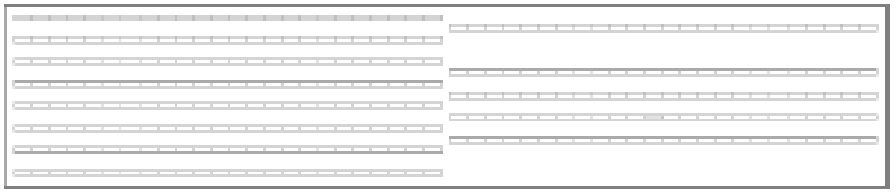

19.78-A

19.82

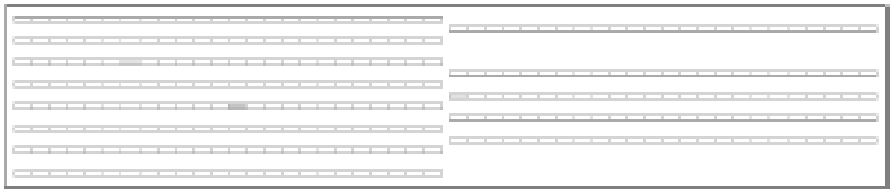

19.83

19.87

12.62 (Run № 2746)

19.62 (Run № 2856)

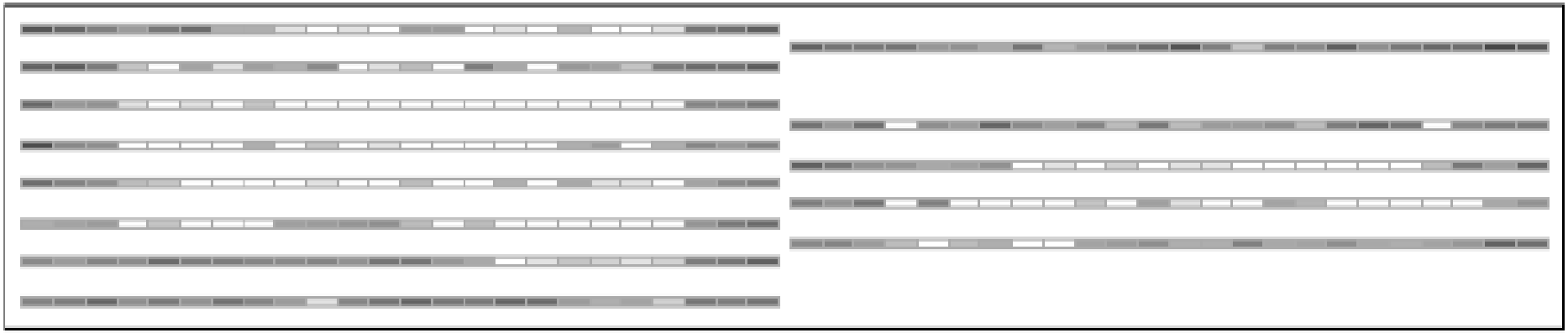

Fig.6. Examples of large nuclear cascades in calorimeter.

- Only 10 out of 110 events have no accompanying hadrons in the calorimeter (EK <~ 2.0•10^-5. The axes of 6 of these events are at large distances from the calorimeter (>~ 10 m). It is not excluded however, that at least some part of hadron less events is initiated by primary gamma-quanta (criteria of the possible gamma-EAS selection are discussed in [3]).

2. Comparison of fit level FF to NKG distribution for the observed events, with that for the events outside the series. Before the observation of the series, by the work on fitting of EAS to NKG function, it was found that the distribution of FF is located in the borders 0.02 <= FF <= 0.12 and has a two-hump form - with maximums at the fit levels FF=0.03 and FF=0.07, with a distinct trough between them and with the maximal value of FF = 0.12. This distribution for $N_e > 10^6$ is shown in Fig. 7.

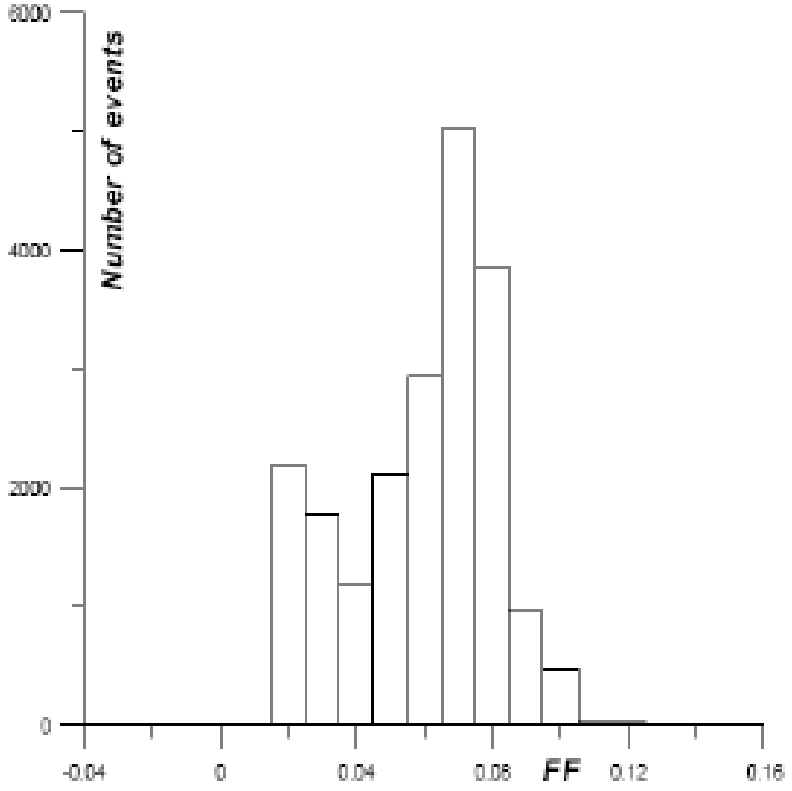

Рис. 7. Distribution of squared deviation FF of NKG function from experimental spatial distribution in the individual EAS outside the series for $N_e > 10^6$.

- **The events of the series in whole diapason Ne >~ 10^6 – 10^9 form a completely analogous distribution of FF with domination in the region of the second maximum, i.e. around of FF=0.07, like the events of the analogous energies outside the series, not crossing the limits, characteristic for the “ordinary” EAS – see the Tables of data for series.**
- **What defines the two-hump character of this distribution is not clear yet. It seems to be natural to explain the presence of the second hump by the contribution of more energetic EAS, which may have several secondary axes. These EAS naturally do not fit so well. The main thing here is that the fit level of the EAS of series does not exceed that of the ”ordinary” EAS.**

3. In ~70% of cases, the quality of the events in the calorimeter makes it possible to estimate the spatial angle of the EAS registration, independently from the chronotron part of the installation. For about 50 events, it is possible to estimate the spatial angle by means of both methods simultaneously – through the chronotron and through the hadron component data in the calorimeter.

- **We stress, that these two approaches are completely independent, both in the sense of device and of the measurement method.**

- **In Fig.8 the distribution of the differences of the zenith angles obtained via these 2 methods in parallel is shown. In the majority of cases, the closeness of the results obtained by means of these two methods is obvious.**

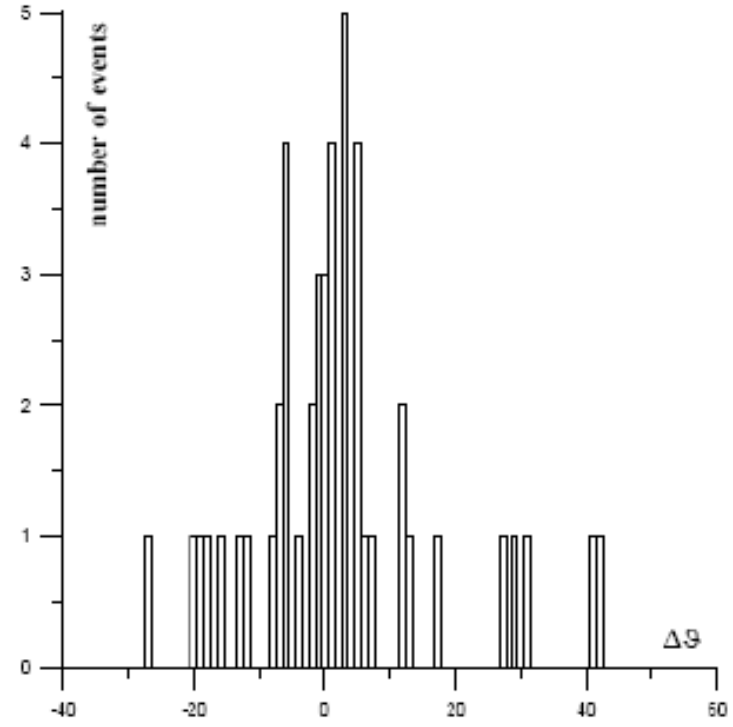

Fig .8. The distribution of the differences of the zenith angles, measured via the chronotron and via the hadron component data in the calorimeter in parallel, for the angular diapason $20^0 - 60^0$

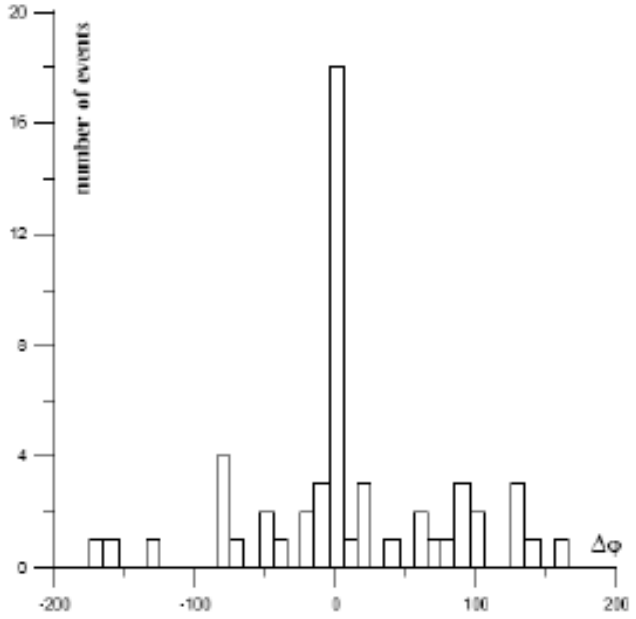

Fig. 9. The distribution of the differences of the azimuth angles measured via the chronotron and via the hadron component data in the calorimeter in parallel. (The events are the same, as in Fig.8).

- **So there are all reasons to be certain, that the observed events are of good quality by all parameters; the behavior of their hadron and electron components corresponds each to other and to commonly accepted characteristics:**

- **and so these events evidently are true Extensive Air Showers.**

- **Note, that 1 series of Gamma - EAS in the region of relatively low energies Ne ~ 10**15 eV was observed in the University of Manitoba [4]. The event was registered at 20.01 1981. Unfortunately there are no experimental data from our installation for this data at our disposal.**

THE MAIN CONCLUSIONS

1. **It is essential, that the frequency of the appearing of such series is much higher, than the probability of the occasional fluctuations in the succession of independent EAS.**

This is in favor of the commonality of their origin.

2. Apparently, the majority of events in these series are initiated by the charged particles, and not by the gamma quanta. This is indicated by asymmetry of the galactic coordinate distribution of the axes directions of EAS, composing these series.

3. The approach described may serve as an additional method for the search of cosmic radiation sources, and for the independent evaluation of magnetic fields distribution in the Galaxy.

4. We do not discuss the possible nature of the phenomenon described.

If one supposes that EAS of the series were emitted isotropic from the source, the source must be taken as being located close to the Earth (at the distance of the order of several thousands of light years). Otherwise unlikely huge energies must have been emitted.

But it is possible to suppose the jet-like character of the emission.

5. The possibility seems to be extremely interesting and important, that at least the part of the described series could be observed *on the other installations at the quoted dates and time. In this case it would be useful to carry on further investigations with joint efforts.*

6. In particular it could be possible to use the analogous data from other installations to search for synchronous events in our material.

THE PEQULIARITIES OF EAS MUON AND HADRON COMPONENT SPECTRA

"CHANGE OF PRIMARY COSMIC RAY NUCLEAR COMPOSITION IN THE ENERGY RANGE 1015 – 10**17 eV AS A RESULT OF THE INTERACTION WITH THE INTERSTELLAR COLD BACKGROUND OF LIGHT OBJECTS (PARTICLES)"**

T.T.Barnaveli* , T.T.Barnaveli (jr), N.A.Eristavi, I.V.Khaldeeva

Tbilisi Institute of Physics, Georgian Acad. Sci., Tamarashvili 6, Tbilisi 380077, Georgia

- **This result was obtained in 1990-es, first based on the EAS mu component study (multiple muons - energy and intensity).**
- **Then investigation was continued by means of EAS hadronic component properties. Recently a new perspective possibilities emerged, so the investigations are renewed again.**

Published:

[1] T.T.Barnaveli, I.V.Khaldeeva, Z.T.Shergelashvili, N.A.Eristavi Phys. Lett., B 346 (1995) 178.

[2] T.T.Barnaveli, T.T.Barnaveli (jr), A.P.Chubenko, N.A.Eristavi, I.V.Khaldeeva, N.M.Nesterova and Yu.G.Verbetsky, Phys. Lett., B 369 (1996) 372.

[3] T.T.Barnaveli, T.T.Barnaveli (jr), N.A.Eristavi, I.V.Khaldeeva, and Yu.G.Verbetsky, Phys. Lett., B 384 (1996) 307.

[4] T.T.Barnaveli, T.T.Barnaveli (jr), N.A.Eristavi, I.V.Khaldeeva, and Yu.G.Verbetsky, in Very high Energy Phenomena in the Universe. Rencontres de Moriond, (1997) 419.

[5] T.T.Barnaveli, T.T.Barnaveli (jr), A.P.Chubenko, N.A.Eristavi, I.V.Khaldeeva, N.M.Nesterova and Yu.G.Verbetsky. Arxives, astro-ph / 0208275

The specific energy *Eh(Ne)/Ne* of the EAS hadronic component for different configurations of installation and selection conditions

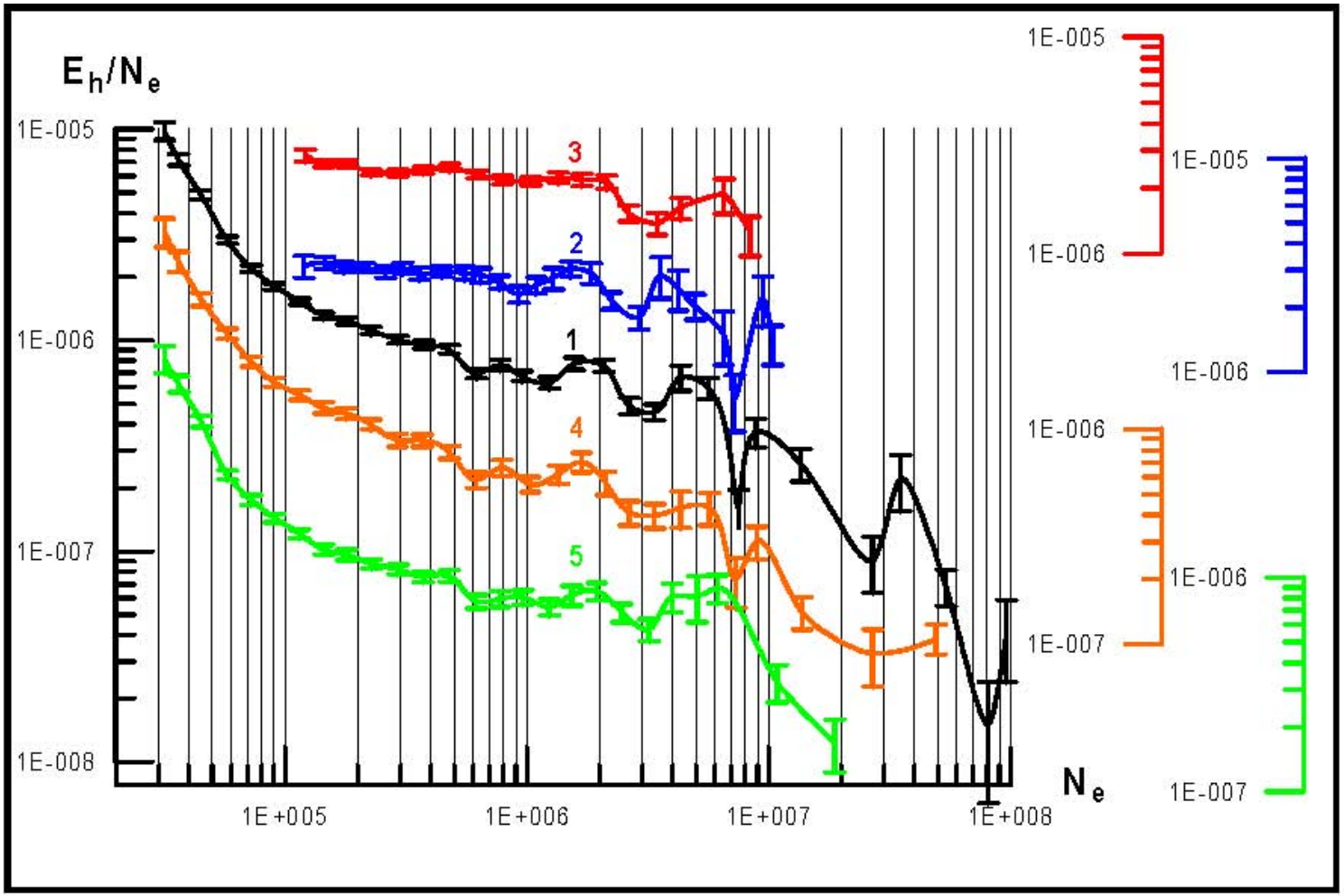

The indicated dips in *Eh(Ne)/Ne* dependence are located in the regions of the same values of *Ne* , regardless of experimental material used and of triggering and selection conditions (curves 1,2 and 3).

The localization of these dips does not depend on the zenith angle of the event registration (curves 4 and 5 – the angles 0 – 20 and 20 – 30 degrees respectively).

- **These peculiarities are difficult to be explained via known astrophysical mechanisms of particle generation and acceleration.**

- **In the basis of the model explaining from the united positions all these peculiarities of hadron *Eh(Eo)/Eo* (and muon *Eμ(Eo)*) component specific energy fluxes the destruction of the Primary Cosmic Radiation (PCR) nuclei *on some monochromatic background of interstellar space, consisting of the light objects of the mass in the area of 36 eV (maybe the component of a dark matter) [1] – [5].***

- **The destruction thresholds of PCR different nuclear components correspond to the peculiarities of *Eh(Eo)/Eo.***

- **The experimental results are in good agreement with the Monte-Carlo calculations carried out in the frames of the proposed model.**

The essence of the deep formation mechanism on *Eh(Ne)/Ne* dependence

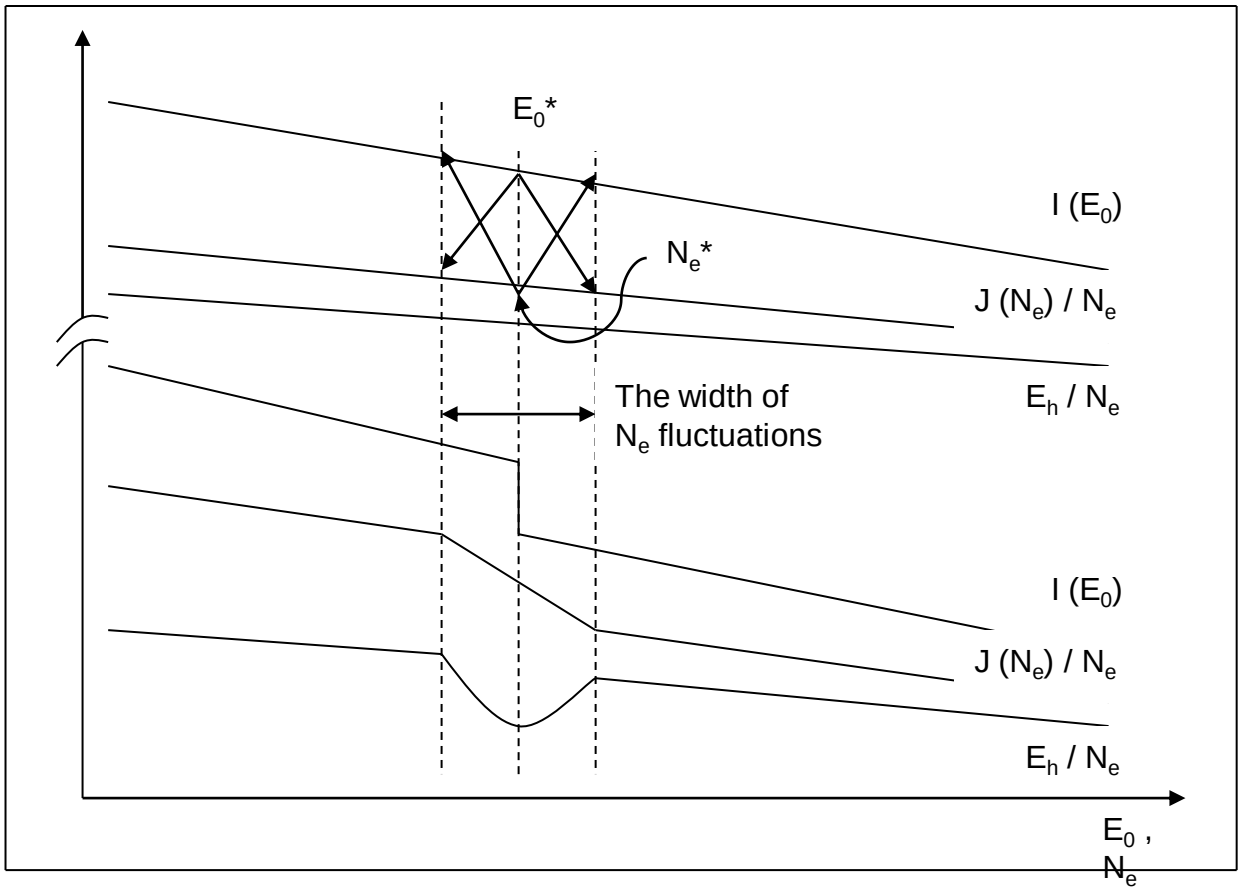

- Let the spectrum of the certain component of PCR have the form $I(E) = K \cdot E^{*}(-r)$. Now let at primary energies higher then Eo^{*} the flux of this component of PCR sharply decreases (the value of coefficient K falls sharply). However the spectrum $J(E)$ of the corresponding EAS will not be cut off above the value Ne^{*} since the showers from primary particles of the energies $Eo < Eo^{*}$ will still be registered due to fluctuations of Ne in the showers of total energy $Eo < Eo^{*}$. The showers initiated by the primary particles (of the PCR component under consideration) of the energy $Eo > Eo^{*}$ will be present to the extent of the new value of coefficient K.

The curve 1 and the downward directed arrows – the correspondence between the deeps on the dependence *Eh(Ne)/Ne* and the thresholds of PCR nuclei destruction.

The upward directed arrows – the low energy border of the area of PCR fragments accumulation.

The curve 2 – the Monte-Carlo calculation

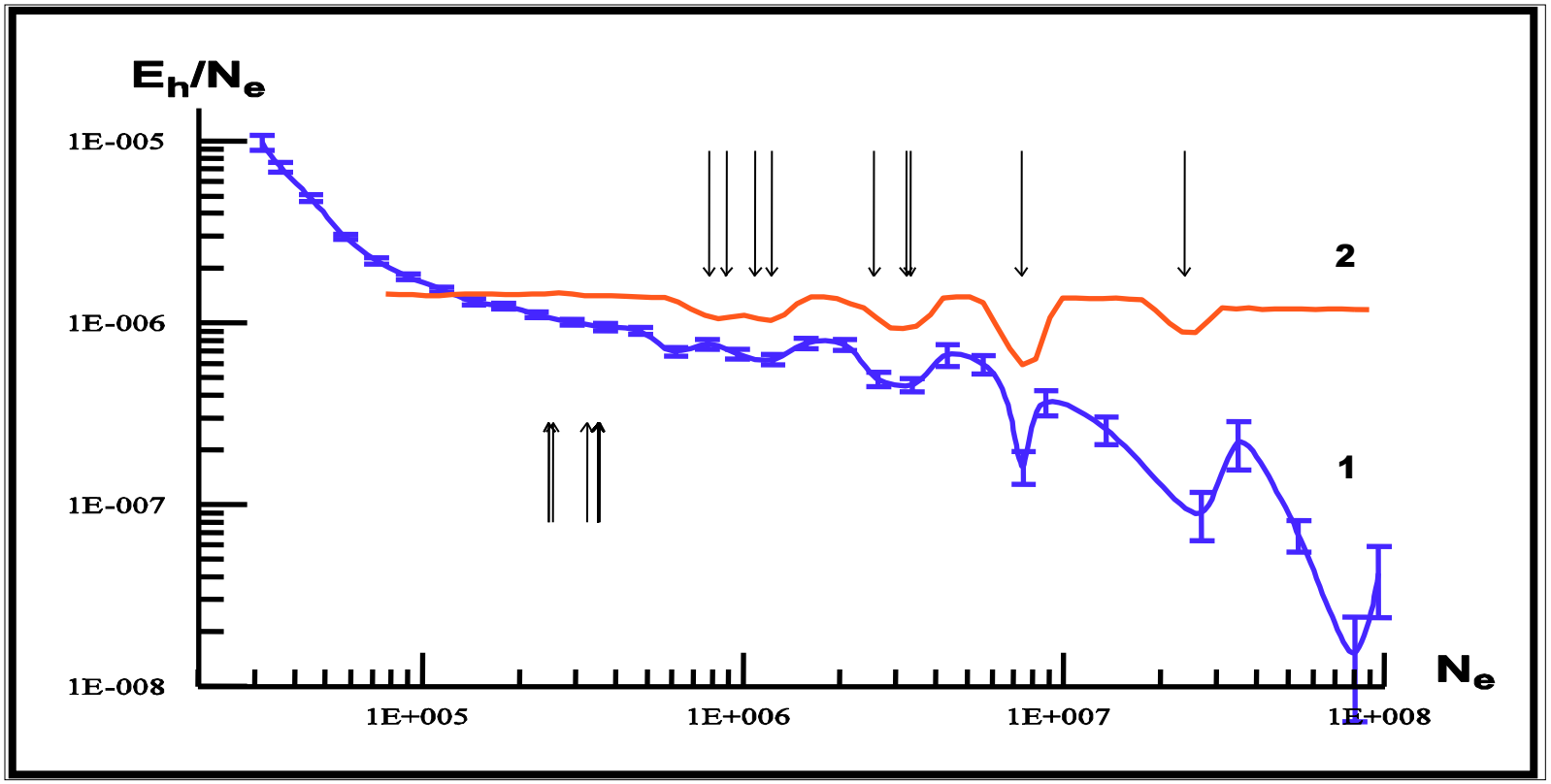

Now we have some new idea of continuation of this research by means of cosmic Rays.

But will it be possible to check this result *by means of accelerator* ? The main idea was to search for the interaction with the vacuum of accelerator tube – these light objects will penetrate inside, like neutrinos. But the vacuum inside tube is too bad *for this task*, it will cause the huge background. The question is: may be in some separated part of the tube (with very thin mailar-like film) it will be possible to reach the needed degree of vacuum – the difference of pressures will be small even for a large film. I do not know, but if possible – the temptation is very high.

? ? ? ? ? ? ? ? ? ? ? ? ? ?

?

Will it be possible?